International Journal of Solids and Structures (vol. 230-231): November 2021

**DOI**: https://doi.org/10.1016/j.ijsolstr.2021.111171

International Journal of Solids and Structures

# Limitations in the design of deployable structures with straight scissors using identical elements

--Manuscript Draft--

| | |
|---|---|
| Manuscript Number: | IJSS-D-20-00854R2 |
| Article Type: | Research paper |
| Keywords: | Geometry; Deployable structure; Scissor; Mechanism; Folding; Kinematics; Identical element; Identical length; Identical cross section |
| Corresponding Author: | Carlos Jose Garcia Mora, M.S.<br>Sevilla University, Higher Technical School of Architecture of Sevilla (ETSAS)<br>Sevilla, Sevilla SPAIN |
| First Author: | Carlos Jose Garcia Mora, M.S. |
| Order of Authors: | Carlos Jose Garcia Mora, M.S. |
| | Jose Sánchez-Sánchez, Professor of Architecture |
| Abstract: | After the recent publications on the design of deployable structures with straight scissors, it has been shown that the possibilities in the application of this type of structure are enormous: organic geometries, bistability control, etc. However, one of the aspects that have still not been studied is the particular case of using identical elements. On the one hand, the satisfaction of this geometric condition implies advantages in the structural behaviour and in the manufacturing and assembly process, but, on the other hand, this geometric constraint also limits design possibilities as will be demonstrated in this paper. Consequently, this research will develop a mathematical process to demonstrate that only non-bistable planes, non-bistable cylinders with a circle base and non-bistable spheres can be designed as deployable if straight scissors and identical elements are used. |

# Limitations in the design of deployable structures with straight scissors using identical elements


| Corresponding Author | |
|---|---|
| Full name | Carlos José García Mora |
| Name in scientific papers | Carlos J. García - Mora |
| Affiliation | Architecture School of Seville University, Spain (PhD candidate)<br>Department of Building Structures and Geotechnical Engineering |
| Phone | +34 671 93 25 15 |
| E-mail address | email@carlosjosegarciamora.com |

| Co-author | |
|---|---|
| Full name | Jose Sánchez Sánchez |
| Name in scientific papers | Jose Sánchez - Sánchez |
| Affiliation | Architecture School of Seville University, Spain (Professor)<br>Department of Building Structures and Geotechnical Engineering |



## Abstract

After the recent publications on the design of deployable structures with straight scissors, it has been shown that the possibilities in the application of this type of structure are enormous: organic geometries, bistability control, etc. However, one of the aspects that have still not been studied is the particular case of using identical elements. On the one hand, the satisfaction of this geometric condition implies advantages in the structural behaviour and in the manufacturing and assembly process, but, on the other hand, this geometric constraint also limits design possibilities as will be demonstrated in this paper. Consequently, this research will develop a mathematical process to demonstrate that only non-bistable planes, non-bistable cylinders with a circle base and non-bistable spheres can be designed as deployable if straight scissors and identical elements are used.



**Keywords:** Geometry; Deployable structure; Scissor; Mechanism; Folding; Kinematics; Identical element; Identical length; Identical cross section

## 1. Introduction:

Deployable structures are mechanisms that have the property to be folded in a compact module when its transport or storage is required and they will be deployed in the destination place. Due to the importance of this type of structures, numerous researchers and designers have developed novel methods to achieve a better prediction of the behaviour of the structure during the deployment process [1] [2] [3].

Although the world of deployable structures is enormous, a basic classification based on deployable structures of plates and deployable structures of elements can be proposed. The first group is composed of the deployable Origami (the deployment is obtained bending the surface) [4] [5] [6] and the deployable Kirigami (the deployment is obtained cutting the surface) [7] [8]. The most important property of these structures is that the joints are lines instead of points and the most famous example of deployable Origami is the Miura pattern where a flat shape can be folded in a small package (Fig. 1).

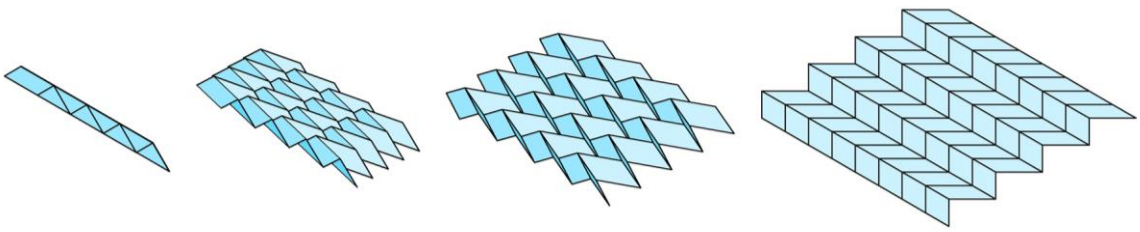

**Fig. 1.** Deployment process of a flat Miura pattern.

The second group is composed of the deployable grid systems [9] [10] and the deployable scissor systems [11] [12] [13] (this paper will be focused on the scissor mechanisms). Basically, the scissors mechanisms are a crank mechanism [14] [15] with a geometric extension of the axes of all elements and this extension is going to be used to connect the next scissor and to get a transmission of the movement: Fig. 2

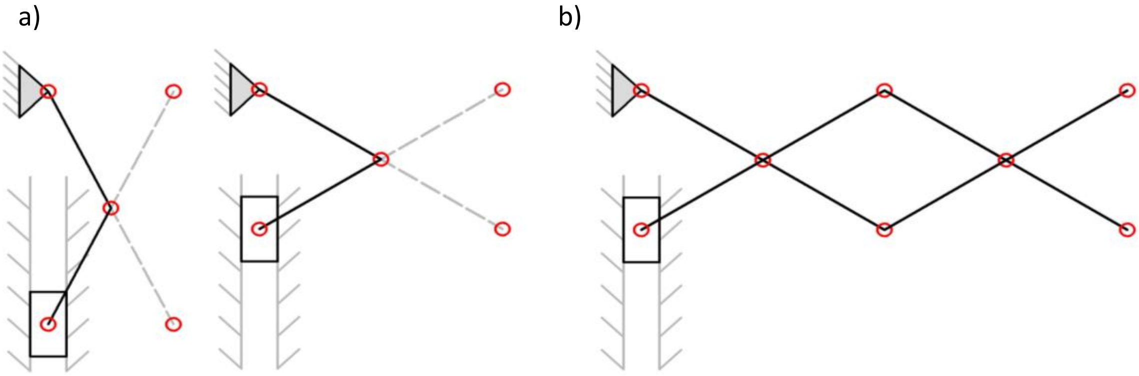


**Fig. 2.** (a) Basic crank mechanism; (b) Scissor mechanism based on a crank mechanism.

An application of this design strategy can be obserbed in Figure 3, where a deployable surface using translational units [16] [17] has been designed to cover a space. The deployment process of the structure is an important aspect that must be considered during the design process to evaluate possible collisions between the scissors.

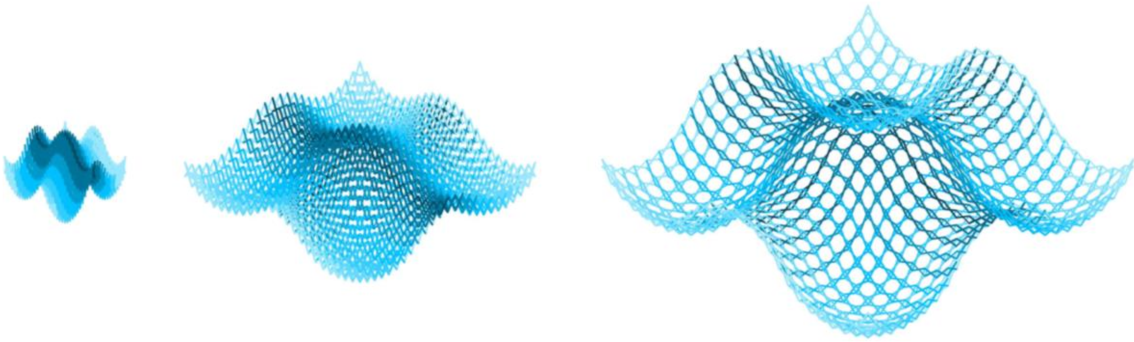

**Fig. 3.** Deployment process of a surface using translational units.

Another parameter that is usually considered to clasificate the deployable structures with scissors is the bistability. In function of this property, two types of structures can be created: Bistable and non-bistable.

The main difference between both is the existence of a geometric incompatibility during the deployment process. In non – bistable structures, this incompatibility is null and there are no forces in the elements during the deployment process due to the elastic deformation. However, in bistable structures [18] [19] [20], there is a geometric incompatibility during the deployment process with an elastic deformation of the elements. This situation means that the structure is going to have two positions of stability: the folded position and the unfolded position.

Despite of the wide range of design possibilities (bistability, angle between the elements [21] [22] [23] [24], etc.), a question that has not still answered in the deployable structure world is the following: Which types of deployable structures can be obtained if the length of all elements is identical? and, are there infinite design possibilites or just a few design options?. The interest in this geometrical constraint is because this property can provide the following advantages:

a) The natural frequencies of the structure will be higher: the use of elements with an identical length will allow the creation of deployable structures with a higher stiffness and, in consequence, with less horizontal displacements.

b) The manufacturing and construction process may be simpler when the length of the elements is a critical point: the worker does not need to change the cut length of the elements and its transport would be easier. However, the position of the middle joint will be different in each element and, in consequence, necessary measures must be taken in order to avoid an incorrect orientation of the elements.

Two designers who have already proposed this type of structures were Félix Escrig Pallarés and Jose Sánchez Sánchez. These authors manufactured a certain quantity of elements with the same length and with an excentricity in the middle joint. The connection of these elements gave the final geometry. A result of their works can be observed in Fig. 4, where a sphere with elements of the same length has been designed (the cables are attached after the deployment process).

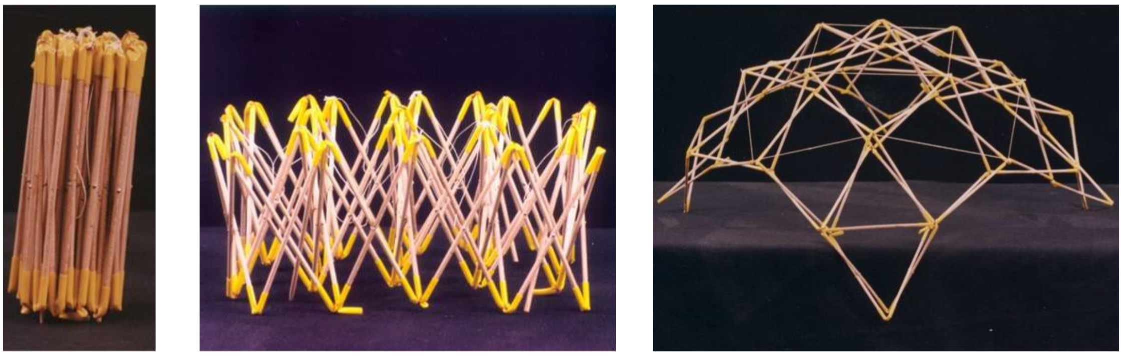

**Fig. 4.** Model of a sphere with elements of the same length and with cables to get rigidization.

Consequently, the goal of this paper will be to obtain the bistable and non-bitable geometries that can be designed as depoyable if the next condition is established: The length of all elements must be the same in all scissors of the structure. It is important to highlight that the work of this research is not a method to design deployable structures and what is going to be developed here are the shapes that can be created having in consideration this geometric constraint.

## 2. Methodology:

The methodology that is going to be developed in this research is the following:

- Step 1: The geometric constraints that scissors with same length elements must satisfy will be imposed. This section is going to be called: “Mathematical development”.

- Step 2: The geometric constraints of step 1 will be applied to a curve and the limits in the design of the deployable curve will be obtained. This section is going to be called: “Application to a curve”.

- Step 3: The geometric constraints of step 1 will be applied to a surface and the limits in the design of the deployable surface will be obtained. This section is going to be called: “Application to a surface”.

- Step 4: A comparison between a deployable structure with indentical elements and a deployable structure with different length of the elements will be developed. This section is going to be called: “Results”. The goal is to discover which advantages and disadvantages have the use of identical elements in terms of structural behaviour (vertical deformations and natural frequencies).

## 3. Mathematical development:

The situation of geometric convergence where the cross point between the elements is in the tangency point between the ellipses has been represented in Fig. 5.

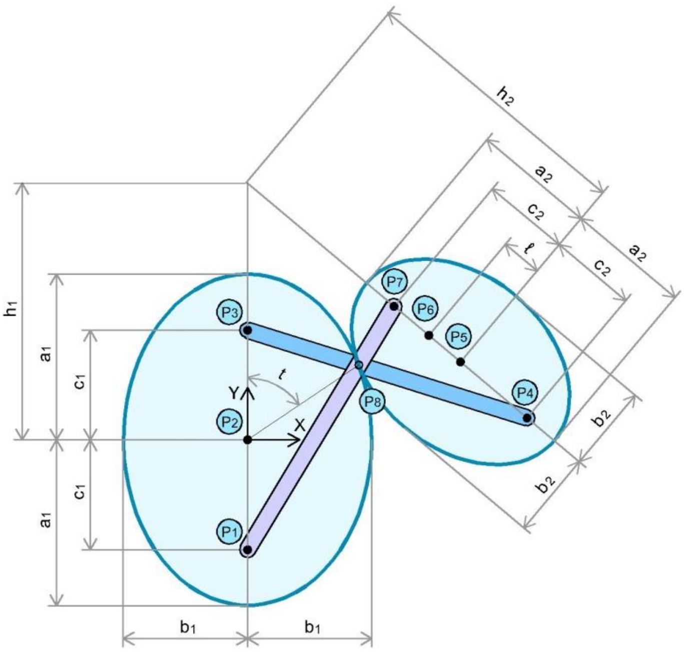


**Fig. 5.** Convergence situation for two ellipses in the plane.

$$P_1 = (0, -c_1) \tag{1}$$

$$P_2 = (0,0) \tag{2}$$

$$P_3 = (0, c_1) \tag{3}$$

$$P_8 = \left(\frac{\sin(t)}{k}, \frac{\cos(t)}{k}\right) \text{ (parametric equation of an ellipse)} \tag{4}$$

Where:

$$k = \sqrt{\left[\frac{\cos(t)}{a_1}\right]^2 + \left[\frac{\sin(t)}{b_1}\right]^2} \qquad \text{with } 0 \leq t \leq 2 \cdot \pi \tag{5}$$

In addition, the geometric conditions of Fig. 6 and Fig. 7 must be satisfied:

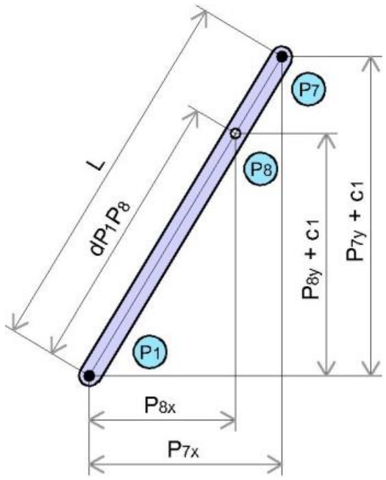


**Fig. 6.** Distance between points in the element $P_1P_8P_7$.

$$\frac{P_{7x}}{P_{8x}} = \frac{L}{dP_1P_8} \rightarrow P_{7x} = P_{8x} \cdot \frac{L}{dP_1P_8} \quad \text{with } L = \text{Length of the element } P_1P_8P_7 \tag{6}$$

$$\frac{P_{7y}+c_1}{P_{8y}+c_1} = \frac{L}{dP_1P_8} \rightarrow P_{7y} = \left(P_{8y}+c_1\right) \cdot \frac{L}{dP_1P_8} - c_1 \quad \text{with } L = \text{Length of the element } P_3P_8P_4 \tag{7}$$

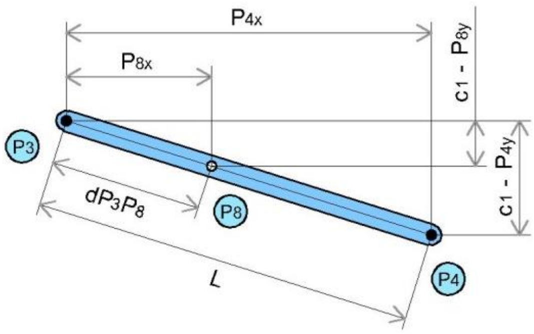


**Fig. 7.** Distance between points in the element $P_3P_8P_4$.

$$\frac{P_{4x}}{P_{8x}} = \frac{L}{dP_3P_8} \rightarrow P_{4x} = P_{8x} \cdot \frac{L}{dP_3P_8} \tag{8}$$

$$\frac{c_1 - P_{4y}}{c_1 - P_{8y}} = \frac{L}{dP_3P_8} \rightarrow P_{4y} = \left(P_{8y}-c_1\right) \cdot \frac{L}{dP_3P_8} + c_1 \tag{9}$$

Consequently:

$$P_4 = \left(P_{8x} \cdot \frac{L}{dP_3P_8}, \left(P_{8y}-c_1\right) \cdot \frac{L}{dP_3P_8} + c_1\right) \tag{10}$$

$$P_7 = \left(P_{8x} \cdot \frac{L}{dP_1P_8}, \left(P_{8y}+c_1\right) \cdot \frac{L}{dP_1P_8} - c_1\right) \tag{11}$$

Then:

$$P_5 = \left(\frac{P_{4x} + P_{7x}}{2}, \frac{P_{4y} + P_{7y}}{2}\right) \tag{12}$$

$$P_6 = \left(P_{5x} + \Delta l_x, P_{5y} + \Delta l_y\right) = \left(\frac{P_{4x} + P_{7x}}{2} + \Delta l_x, \frac{P_{4y} + P_{7y}}{2} + \Delta l_y\right) \tag{13}$$

On the other hand:

$$dP_3P_8 = \sqrt{\left[\frac{\sin(t)}{k}\right]^2 + \left[\frac{\cos(t)}{k} - c_1\right]^2} \tag{14}$$

$$dP_1P_8 = \sqrt{\left[\frac{\sin(t)}{k}\right]^2 + \left[\frac{\cos(t)}{k} + c_1\right]^2} \tag{15}$$

Finally, if Eq. (10), Eq. (11), Eq. (12), Eq. (13), Eq. (14) and Eq. (15) are combined, the equation of the convergence curve is obtained: Eq. (16) and Eq. (17).

$$x(t) = P_{6x}(t) = \frac{n_1 \cdot L}{2} \cdot \left[\frac{1}{\sqrt{n_1^2 + (n_2 - c_1)^2}} + \frac{1}{\sqrt{n_1^2 + (n_2 + c_1)^2}}\right] + \Delta l_x \tag{16}$$

$$y(t) = P_{6y}(t) = \frac{L}{2} \cdot \left[\frac{n_2 - c_1}{\sqrt{n_1^2 + (n_2 - c_1)^2}} + \frac{n_2 + c_1}{\sqrt{n_1^2 + (n_2 + c_1)^2}}\right] + \Delta l_y \tag{17}$$

Where:

$$n_1 = \frac{\sin(t)}{k} \tag{18}$$

$$n_2 = \frac{\cos(t)}{k} \tag{19}$$

The most common design case that can be found is having the centres of all ellipsoids in the surface that is going to be designed as deployable ($P_5$ will belong to the surface). To achieve that, the following values shall be considered: $l = 0 \rightarrow \Delta l_x = 0$ and $\Delta l_y = 0$. The parameters that can be controlled by the designer are: $a_1$, $b_1$ and L ($c_1$ is a function that depends on $a_1$ and $b_1$). Likewise, the L parameter is obtained by multiplying Eq. (16) and Eq. (17). Consequently, the L parameter is going to influence the size of the convergence curve but not its shape. This situation means that the parameters that have an influence on the shape of the curve are just $a_1$ and $b_1$. The relationship between $a_1$, $b_1$ and the shape of the convergence curve for l=0 can be seen in Table 1.

| $b_1/a_1$ | 1 | 0.9 | 0.8 |
|---|---|---|---|
| Convergence curve | 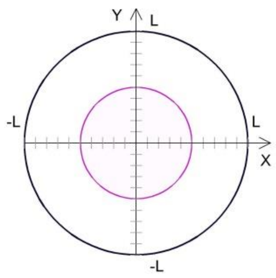 | 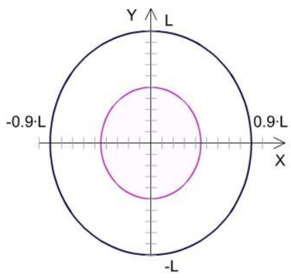 | 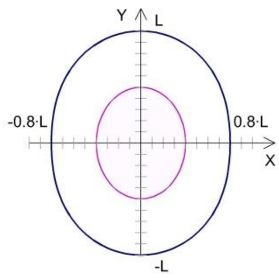 |
| $b_1/a_1$ | 0.7 | 0.6 | 0.5 |
| Convergence curve | 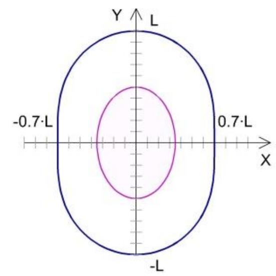 | 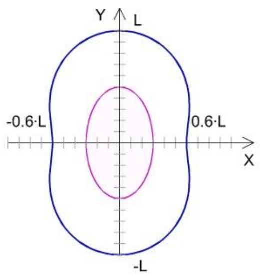 | 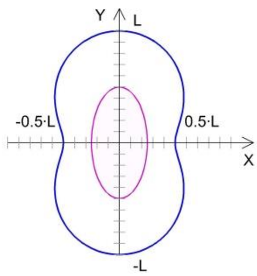 |
| $b_1/a_1$ | 0.4 | 0.3 | 0.2 |
| Convergence curve | 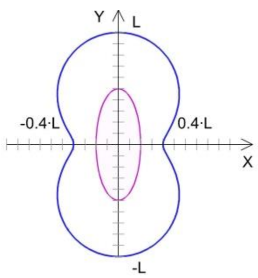 | 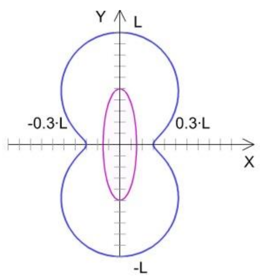 | 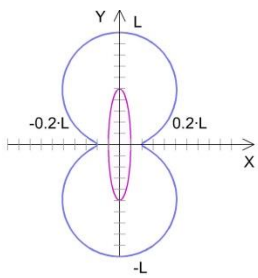 |
| $b_1/a_1$ | 0.1 | 0 | [1,0] |
| Convergence curve | 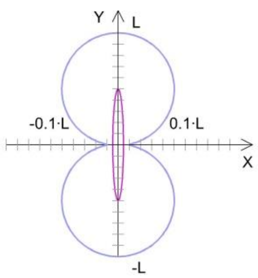 | 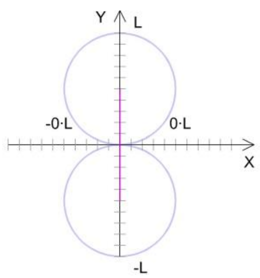 | 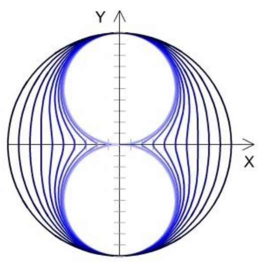 |

**Table 1.** Evolution of the convergence curve in function of $b_1/a_1$ for l = 0.

In the following image, an example of some scissors that belong to the convergence curve can be observed (Fig. 8):

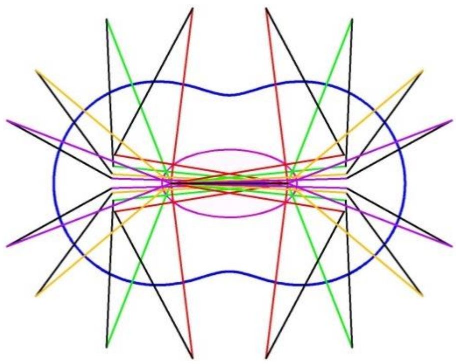

**Fig. 8.** 12 scissors obtained in the convergence curve for $l = 0$ and for $b_1/a_1 = 0.5$ (elements of same colour belong to the same scissor) (elements of all scissors have the same length).

However, the previous design condition has a considerable disadvantage: the final shape will not be the original surface if a textile is hold using the superior or inferior joints of the structure. To solve that, it is necessary that the superior joints ($P_3$ and $P_7$) or the inferior joints ($P_1$ and $P_4$) belong to the original surface. In terms of equations:

- For the first case (superior joints), the next conditions are mandatory: $l = c_2 \rightarrow \Delta l_x = P_{7x} - P_{5x}$ and $\Delta l_y = P_{7y} - P_{5y}$ (Fig. 9)

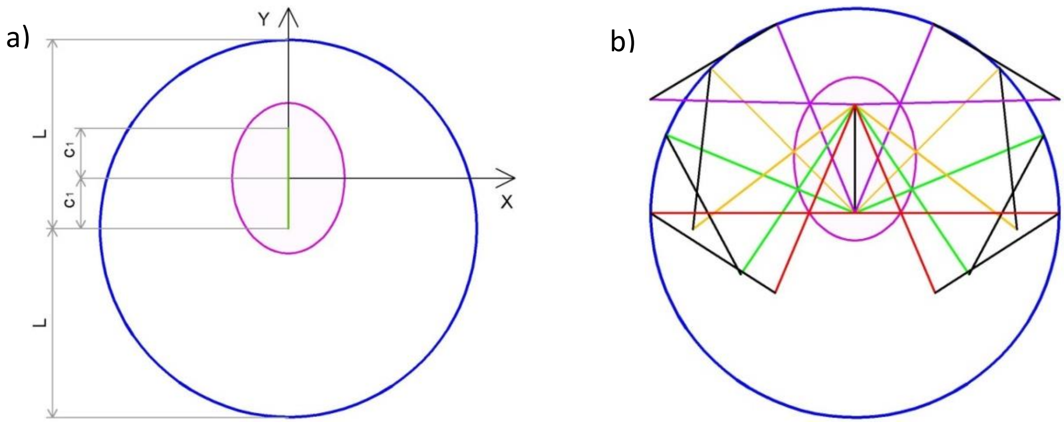


**Fig. 9.** (a) Convergence curve for $l = c_2$ (blue circle with centre in the bottom focus of the original ellipse); (b) 8 scissors that belong to the convergence curve for $l = c_2$

- For the second case (inferior joints), the next conditions are mandatory: $l = -c_2 \rightarrow \Delta l_x = P_{4x} - P_{5x}$ and $\Delta l_y = P_{4y} - P_{5y}$ (Fig. 10)

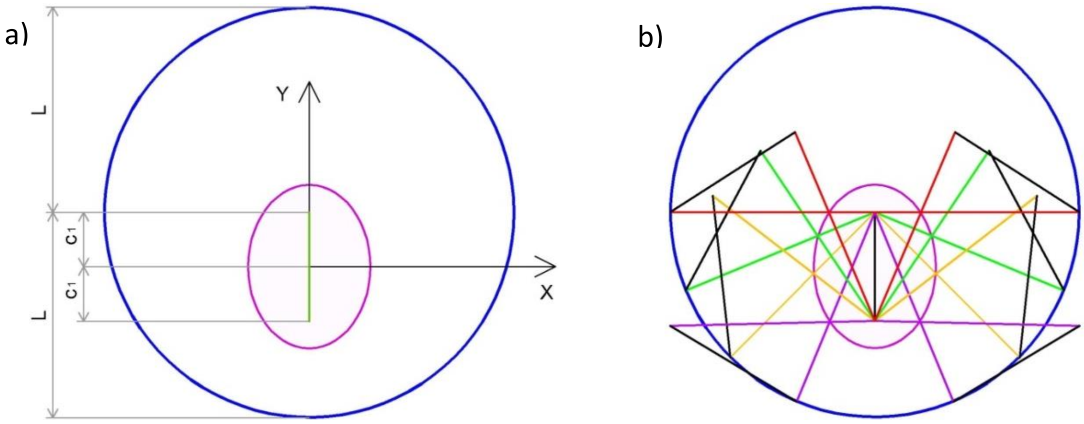


**Fig. 10.** (a) Convergence curve for $l = -c_2$ (blue circle with centre in the top focus of the original ellipse); (b) 8 scissors that belong to the convergence curve for $l = -c_2$

When the convergence curve is obtained for any of the previous cases, the scissor in one point of this curve is going to be defined by 2 parameters: orientation ($h_1$) and the value of the focal distance in the point of the convergence curve ($c_2$):

a) Orientation = $h_1$ (for any value of l parameter):

The line that is defined by $P_4$ and $P_7$ is:

$$y = \frac{P_{4y} - P_{7y}}{P_{4x} - P_{7x}} \cdot x + P_{7y} - P_{7x} \cdot \frac{P_{4y} - P_{7y}}{P_{4x} - P_{7x}} \tag{20}$$

In addition, $h_1 = y(x = 0)$. If this condition is replaced in Eq. (20), Eq. (10) and Eq. (11), the $h_1$ equation is obtained.

b) Focal distance = $c_2$ (for any value of l parameter):

The next equation is obtained from Fig. 5:

$$c_2 = dP_7P_5 = \sqrt{(P_{7x} - P_{5x})^2 + (P_{7y} - P_{5y})^2} = \sqrt{\left(\frac{P_{7x} - P_{4x}}{2}\right)^2 + \left(\frac{P_{7y} - P_{4y}}{2}\right)^2} \quad (21)$$

If Eq. (10) and Eq. (11) are replaced in Eq. (21), the equation of focal distance is obtained. Equations of orientation ($h_1$) and focal distance ($c_2$) will be used in the Chapter 5: Application to a surface.

**4. Application to a curve:**

The first application case that is going to be solved is the situation with l = 0 (the centre of all ellipsoids is in the curve that is going to be designed as deployable) (Fig. 11).

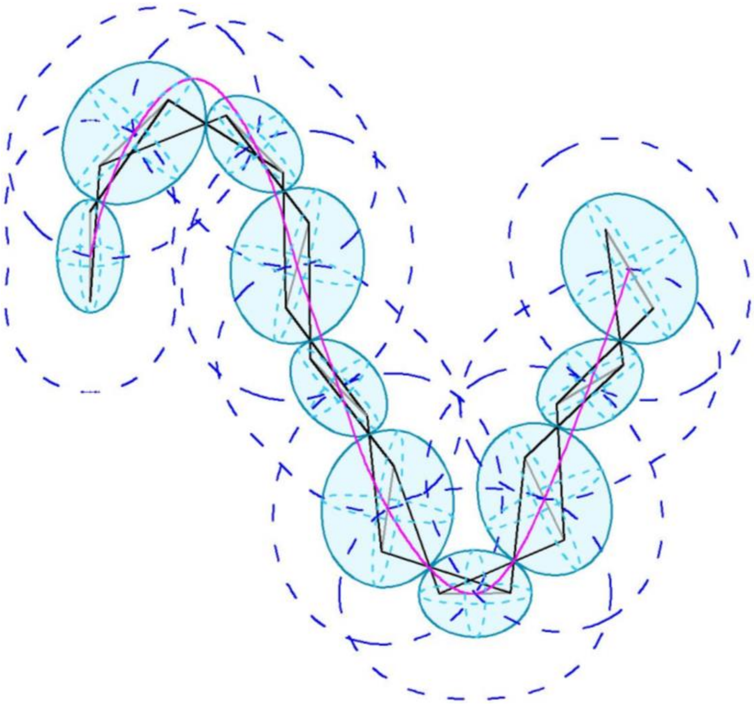

**Fig. 11.** Deployable structure using an identical length in all elements and with l = 0 (purple curve = original curve; discontinuous blue curve = convergence curve).

The second case that will be developed is the situation with $l = c_2$ (the top point of all scissors is going to be in the curve that is going to be designed as deployable) (Fig. 12).

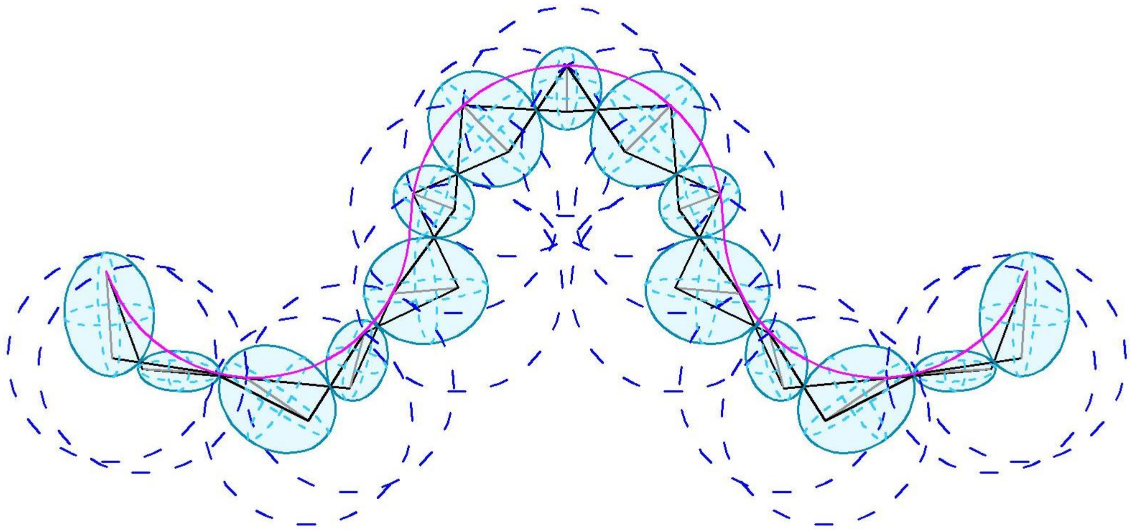

**Fig. 12.** Deployable structure using an identical length in all elements and with l = $c_2$ (purple curve = original curve; discontinuous blue curve = convergence curve).

The last case is the situation with l = -$c_2$ (the bottom point of all scissors is going to be in the curve that is going to be designed as deployable) (Fig. 13).

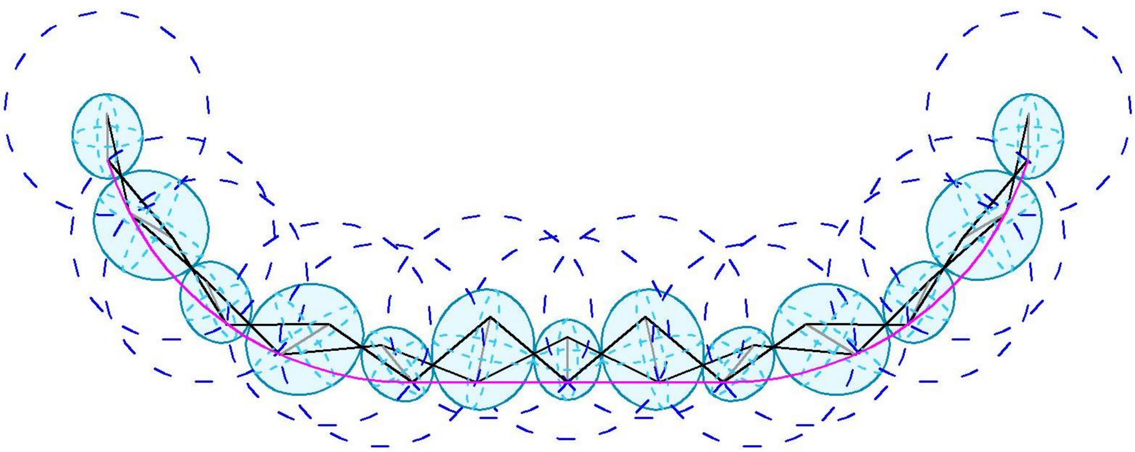

**Fig. 13.** Deployable structure using an identical length in all elements and with l = -$c_2$ (purple curve = original curve; discontinuous blue curve = convergence curve).

## 5. Application to a surface:

The application of this mathematical development to a surface is more complex and, in consequence, the following considerations are going to be taken:

a) When a curve is designed as deployable, the designer always works using one ellipsoid (or ellipse in case of a flat curve). However, when a surface is designed as deployable, the designer always works using two ellipsoids simultaneously in the space. The equation of $c_2$ gives a different value for each point of the convergence surface and when a surface is designed as deployable, $c_2$ must simultaneously have the same value between both original ellipsoids. This situation can only happen in two cases:

a1) Both original ellipsoids are symmetric or they are obtained using a rotation. In this case, the convergence surfaces will be symmetric and the intersection between them will give a curve where all of its points will have the same $c_2$ value between both ellipsoids. The problem is that these geometric conditions hugely limit the design possibilities.

a2) The existence of a relationship between input parameters that allows the creation of a convergence surface where all points will have the same $c_2$ value. This assumption implies that:

$$c_2(t = t_i) = c_2(t = t_{i+1}) \tag{22}$$

Eq. (22) must be satisfied in all points of the convergence surface. In consequence, Eq. (23) can be defined:

$$c_2(t = 0^o) = c_1 = c_2(t = 90^o) = L \cdot \frac{c_1}{a_1} - c_1 \tag{23}$$

Then:

$$c_1 = L \cdot \frac{c_1}{a_1} - c_1 \rightarrow L = 2 \cdot a_1 \tag{24}$$

If Eq. (24) is satisfied:

$$c_2(L = 2 \cdot a_1 \text{ for any value of } t) = c_1 \tag{25}$$

Consequently, if the length of all elements is equal to $2 \cdot a_1$, the $c_2$ value is going to be constant in all points of the convergence surface for any orientation of both original ellipsoids.

Also, an aspect that is important to highlight is that the expression of $c_2$ does not depend on the "l" parameter and, consequently, Eq. (24) and Eq. (25) are going to be satisfied for any value of "l". Finally, the following relationships are satisfied:

$$dP_3P_8 + dP_1P_8 = 2 \cdot a_1 = L = dP_3P_8 + dP_4P_8 = dP_1P_8 + dP_7P_8 \tag{26}$$

$$dP_7P_8 + dP_4P_8 = 2 \cdot a_2 \tag{27}$$

If Eq. (27) is replaced in Eq. (26):

$$2 \cdot L - 2 \cdot a_2 = L \rightarrow L = 2 \cdot a_2 \rightarrow a_1 = a_2 \rightarrow b_1 = b_2 \rightarrow c_1 = c_2 \tag{28}$$

b) Not only $c_2$ value has to be the same between both original ellipsoids, but also the orientation of $c_2$ between both ellipsoids must be the same. This situation means that $h_1$ value between both original ellipsoids must be the same. To study this situation, two cases can be found:

b1) $h_1$ value will be the same between both original ellipsoids if the ellipsoids are symmetric or if they have a relationship of a rotation. However, these geometric conditions hugely limit the design possibilities.

b2) The existence of a relationship between input parameters that allows the creation of a convergence surface where all points will have the same $h_1$ value. This assumption implies that:

$$h_1(t = t_i) = h_1(t = t_{i+1}) \tag{29}$$

Eq. (29) must be satisfied in all points of the convergence surface. In consequence, Eq. (30) can be defined:

$$h_1(t = 0^o) = L - a_1 = h_1(t = 90^o) = c_1 \cdot \left[\frac{L}{a_1} - 1 - \frac{2 \cdot \left(1 - \frac{L}{a_1}\right)}{1 - 1}\right] = \infty \tag{30}$$

The next step is the study of the lateral limits in the previous equation:

$$h_1(t = 90^+) = -\infty \quad \text{and} \quad h_1(t = 90^-) = +\infty \tag{31}$$

The lateral limits are different and, in consequence, the equation does not converge either in + ∞ or - ∞. Consequently, there is not a relationship between the input parameters that allows the existence of a convergence surface where all of their points have the same $h_1$ value.

c) The study will be done for $l = c_2$. "l" is a parameter that allows the control of the tessellation, but it does not guarantee the geometric convergence. Consequently, the following study will give the same results for any value of "l" ($l$ = constant, $l = c_2$ or $l = -c_2$. On the other hand, the use of $l = c_2$ has the following mathematical advantages:

c1) The intersection between both convergence surfaces will be the intersection between two spheres. This situation means that the intersection curve will be a circle.

c2) A sphere has a position in the space but not an orientation. Consequently, the use of a variable to modify the orientation of the convergence surface is not necessary.

d) The angular orientation between both original ellipsoids has an influence on the size of the convergence curve but not on the solution of the convergence (the angular position only implies a rotation and not a displacement).

Once the previous conditions have been established, the goal is to find the set of points in the space that give a scissor with the same orientation between both original ellipsoids (the nonexistence of a mathematical relationship between both original ellipsoids that allows a convergence surface with the same $h_1$ value has been demonstrated before).

This analysis is going to be done using 3 ellipsoids with a rotation of 90º (the results of this study with another angle will be the same due to the relationship of rotation and not of translation). As has been established before, the study will use $l = c_2$ and the centres of the spheres will be in $P_{41}$ and $P_{42}$. The intersection between the convergence surfaces will give the convergence curve (the red and discontinuous curve in the next figure). The final step is to obtain the scissor from each original ellipsoid and the angle between the focal distances of the scissors. When this angle is 0, the orientation value between both original ellipsoids will be the same (Fig. 14).

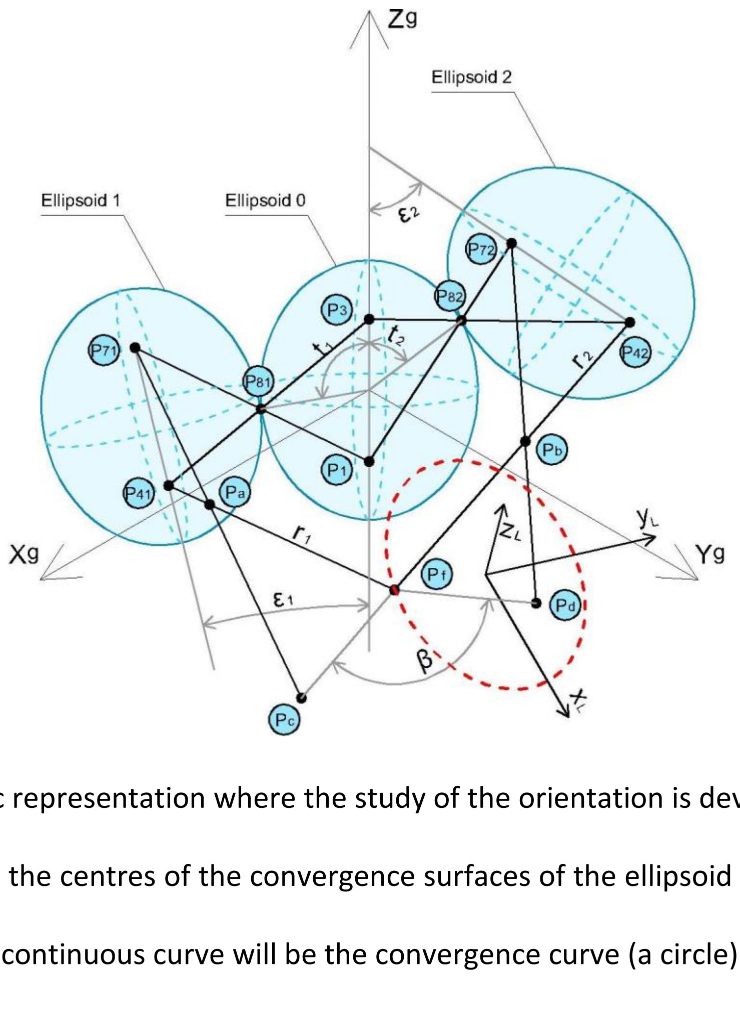


**Fig. 14.** Graphic representation where the study of the orientation is developed (β = 0). $P_{41}$ y $P_{42}$ will be the centres of the convergence surfaces of the ellipsoid 1 and 2 ($l = c_2$). The red and discontinuous curve will be the convergence curve (a circle).

The equations that define the position of $P_{41}$, $P_{71}$, $P_{42}$ y $P_{72}$ have been already obtained in Eq. (10) and Eq. (11). On the other hand, the intersection between two convergence surfaces will be the intersection between two spheres with the same radius (Fig. 15).

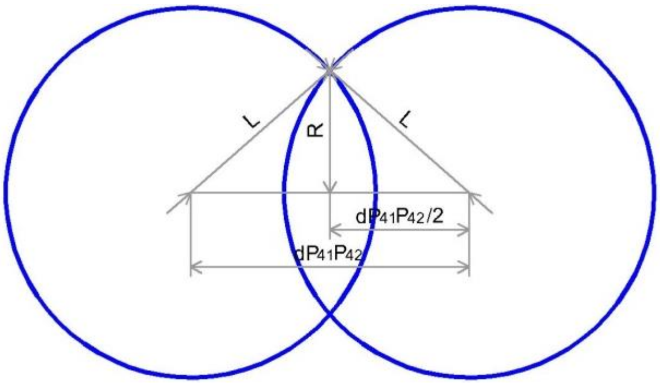


**Fig. 15.** Relationship between the radius of the convergence curve and the convergence surfaces.

Consequently, the radius of the circle will be:

$$L^2 = R^2 + \left(\frac{dP_{41}P_{42}}{2}\right)^2 \rightarrow R = \sqrt{L^2 - \left(\frac{dP_{41}P_{42}}{2}\right)^2} \tag{32}$$

The parametric equation of the convergence curve in local coordinates ($X_L$, $Y_L$, $Z_L$) is:

$$x_L(\gamma) = \sqrt{L^2 - \left(\frac{dP_{41}P_{42}}{2}\right)^2} \cdot \cos(\gamma) \quad \text{with} \quad 0^o < \gamma < 360^0 \tag{33}$$

$$y_L(\gamma) = \sqrt{L^2 - \left(\frac{dP_{41}P_{42}}{2}\right)^2} \cdot \sin(\gamma) \quad \text{with} \quad 0^o < \gamma < 360^0 \tag{34}$$

$$z_L(\gamma) = 0 \tag{35}$$

The goal is to obtain the equation of the convergence curve in global coordinates ($X_G$, $Y_G$, $Z_G$). To achieve that, $Z_L$ must be parallel to the axis of the circle and $X_L$, $Y_L$ can have any orientation due to the infinite planes of symmetry. Also, the orientation of $X_L$ will have a value with the component "Y" equal to 0. This decision will allow the elimination of one of the rotation matrixes in the transformation of a 3D reference system. The final expression of the global coordinates is (the development is demonstrated in appendices):

$$\begin{pmatrix} Pf_{XG} \\ Pf_{YG} \\ Pf_{ZG} \end{pmatrix} = \begin{pmatrix} \frac{P_{41X} + P_{42X}}{2} \\ \frac{P_{41Y} + P_{42Y}}{2} \\ \frac{P_{41Z} + P_{42Z}}{2} \end{pmatrix} + \begin{pmatrix} \cos(\alpha_X) & \sin(\alpha_X)\cdot\sin(\alpha_Y) & -\cos(\alpha_Y)\cdot\sin(\alpha_X) \\ 0 & \cos(\alpha_Y) & \sin(\alpha_Y) \\ \sin(\alpha_X) & -\cos(\alpha_X)\cdot\sin(\alpha_Y) & \cos(\alpha_X)\cdot\cos(\alpha_Y) \end{pmatrix} \cdot \begin{pmatrix} x_L(\gamma) \\ y_L(\gamma) \\ z_L(\gamma) \end{pmatrix} \qquad (36)$$

The next steps will be:

- Step 1: Equations of ellipsoids 1 and 2 in global coordinates.
- Step 2: Definition of the lines $r_1$ and $r_2$.
- Step 3: Intersection between ellipsoid 1 and $r_1$ ($P_a$) and between ellipsoid 2 and $r_2$ ($P_b$).
- Step 4: Line from $P_{71}$ to $P_a$ with a length of L ($P_c$) and line from $P_{72}$ to $P_b$ with a length of L ($P_d$).
- Step 5: Angle between the vectors $\overrightarrow{P_fP_c}$ and $\overrightarrow{P_fP_d}$ (β).

It is important to highlight that the domain of $t_1$ and $t_2$ will be: (0º ,180º] (the value of 0º is not included because the solution is a line and not a scissor). Also, the following study has been developed with L = 2*$a_1$ to guarantee the constant value of the focal distance.

4.1. One "t" value is 90º (in this case $t_2$) and the other "t" value is iterated from 0º to 90º. The values of β and γ for each relationship of $b_1/a_1$ have been represented in Table 2:

| $t_1$=90º and $t_2$=90º | $t_1$=80º and $t_2$=90º | $t_1$=70º and $t_2$=90º |
|---|---|---|
| 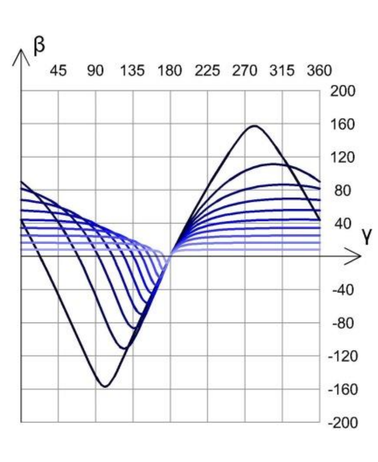 | 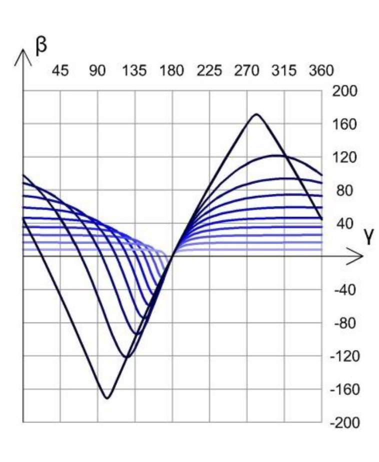 | 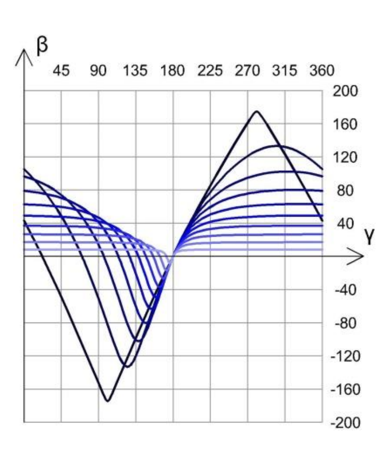 |
| $t_1$=60º and $t_2$=90º | $t_1$=50º and $t_2$=90º | $t_1$=40º and $t_2$=90º |
| 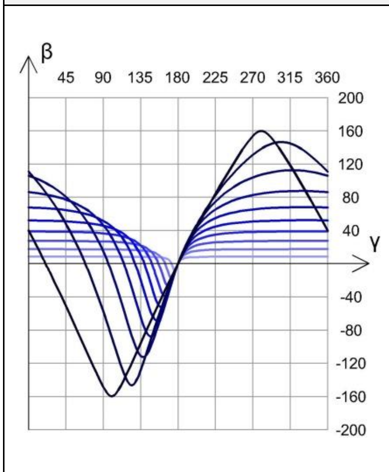 | 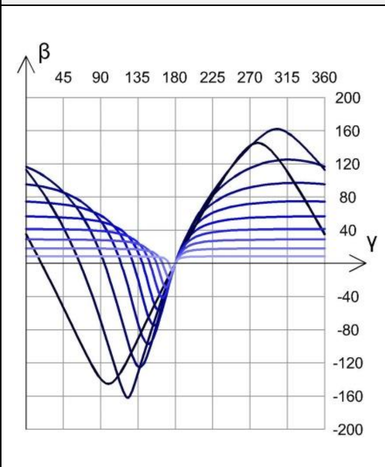 | 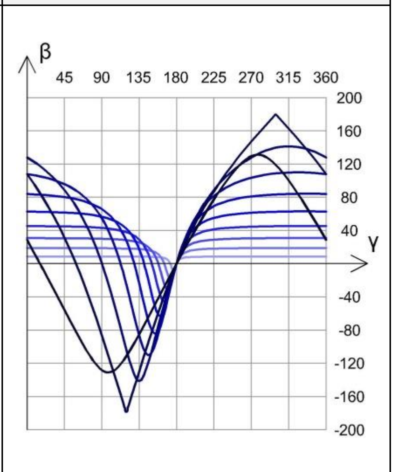 |
| $t_1$=30º and $t_2$=90º | $t_1$=20º and $t_2$=90º | $t_1$=10º and $t_2$=90º |
| 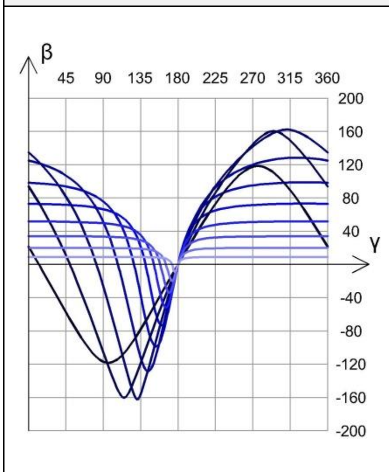 | 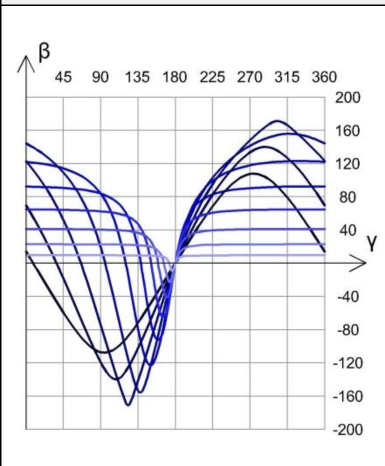 | 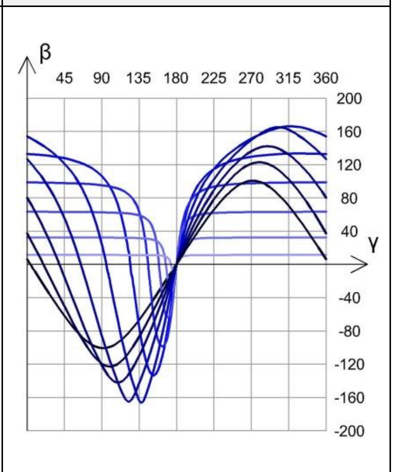 |

| | | | | |
|---|---|---|---|---|
| $b_1/a_1=1$ | $b_1/a_1=0.9$ | $b_1/a_1=0.8$ | $b_1/a_1=0.7$ | $b_1/a_1=0.6$ |
| $b_1/a_1=0.5$ | $b_1/a_1=0.4$ | $b_1/a_1=0.3$ | $b_1/a_1=0.2$ | $b_1/a_1=0.1$ |

**Table 2.** Evolution of the orientation of the scissors with a value of "t" fixed at 90º.

The main property of the Table 2 is the number of times that the graphics cut the horizontal axis (the number of times with β = 0). For these cases, the orientation between ellipsoids 1 and 2 will be the same and there will be a geometric solution. This situation can be represented with the next equation:

$$\text{Number of possible solutions} = (\text{Number of times with } \beta = 0\,) - 1 \quad (1 = \text{trivial solution}) \tag{37}$$

As can be observed in the graphics of Table 2, all curves cut the horizontal axis twice and there will be only one geometric solution. If the geometric solution is drawn for each graphic, the final scissor module is always a perpendicular extrusion with respect to the plane that contains the scissor between ellipsoids 0 and 1. This situation just allows the design of deployable geometries that are the result of a perpendicular extrusion with respect to their generatrix: planes and cylinders with a simple curvature. It is important to highlight that in case of a flat geometry, the condition of $L = 2*a_1$ is not necessary because the scissors only have a relationship of a rotation. However, in the case of a cylindrical geometry, the condition of $L = 2*a_1$ is mandatory because the relationship between the scissors is more than a rotation. Some examples of flat deployable structures with elements of the same length can be observed in Fig. 16, Fig. 17 and Fig. 18.

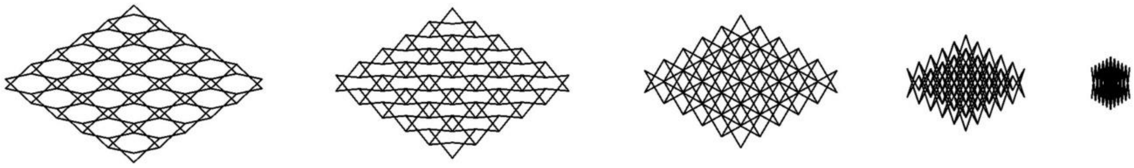

**Fig. 16.** Flat deployable structure with elements of the same length and with a square tessellation.

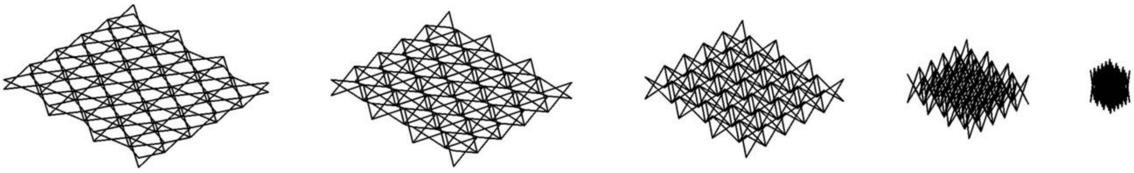

**Fig. 17.** Flat deployable structure with elements of the same length and with a triangular tessellation.

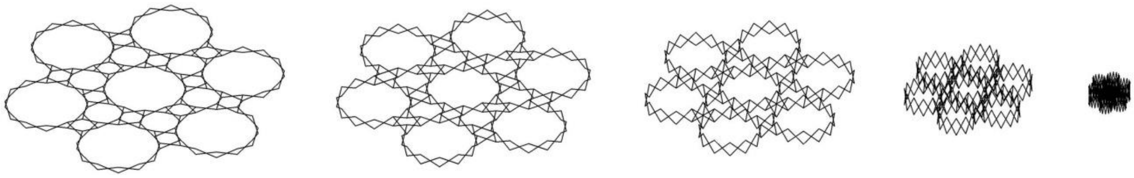

**Fig. 18.** Flat deployable structure with elements of the same length and with a mixed tessellation.

Some examples of a cylindrical deployable structure with a simple curvature and with elements of the same length can be observed in Fig. 19 and Fig. 20.

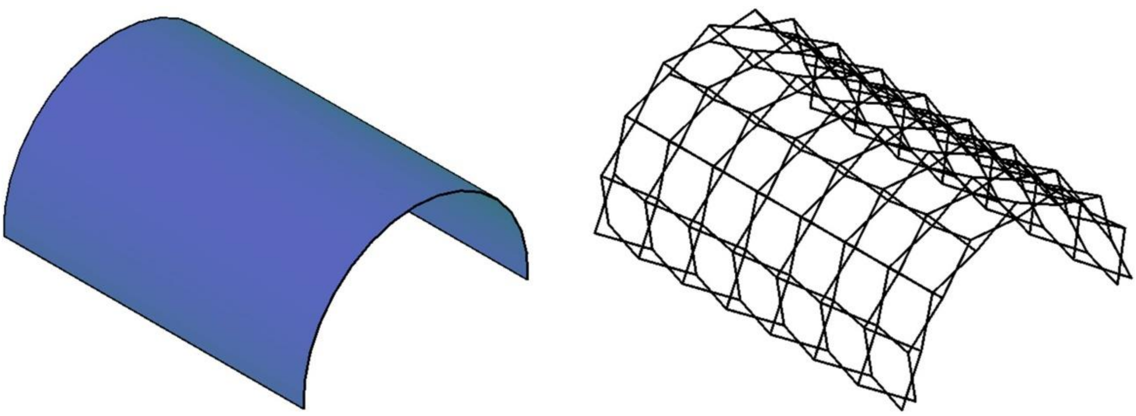

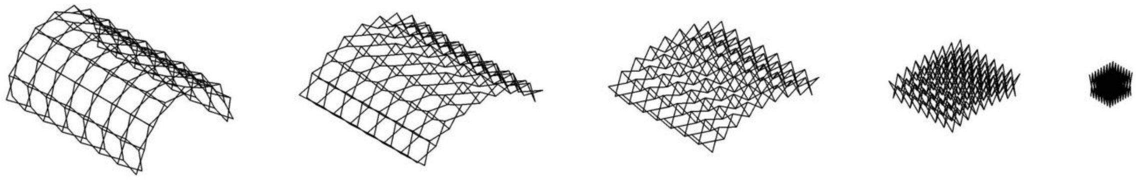

**Fig. 19.** Cylindrical deployable structure with elements of the same length and with a circular generatrix.

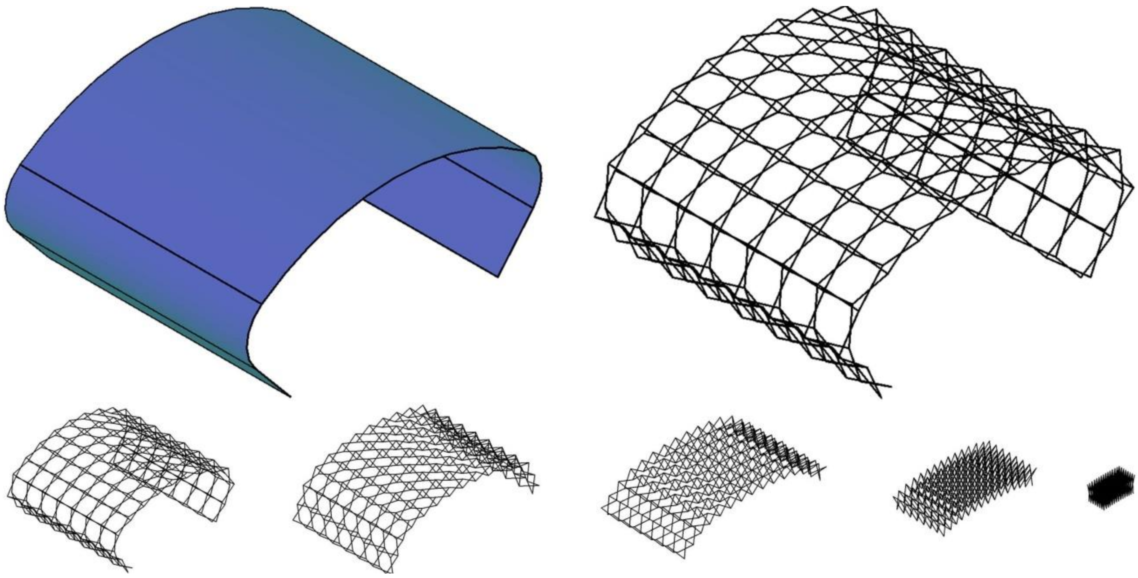

**Fig. 20.** Cylindrical deployable structure with elements of the same length and with a mixed generatrix.

4.2. One “t” value is different in comparison with 90º (in this case $t_2$ = 20 º) and the other “t” value is iterated from 0º to 90º. The values of β and γ for each relationship of $b_1/a_1$ have been represented in Table 3:

| $t_1$=10º and $t_2$=20º | $t_1$=20º and $t_2$=20º | $t_1$=30º and $t_2$=20º |
|---|---|---|
| 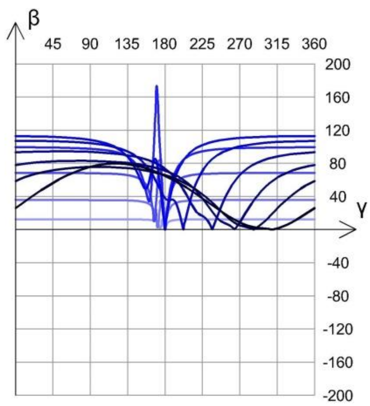 | 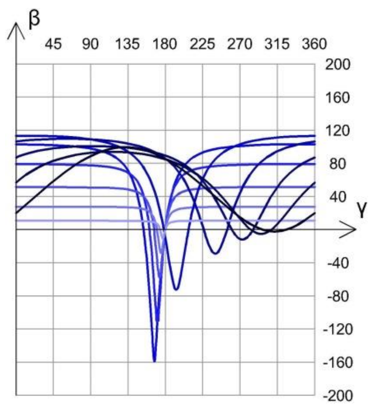 | 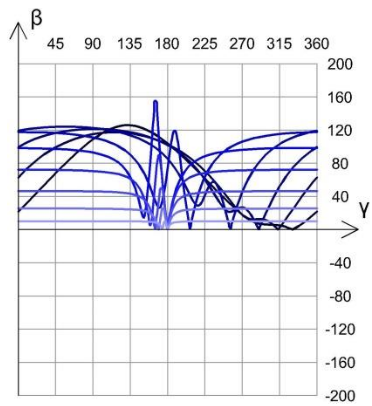 |
| $t_1$=40º and $t_2$=20º | $t_1$=50º and $t_2$=20º | $t_1$=60º and $t_2$=20º |
| 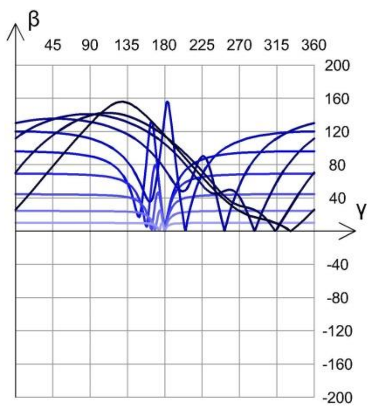 | 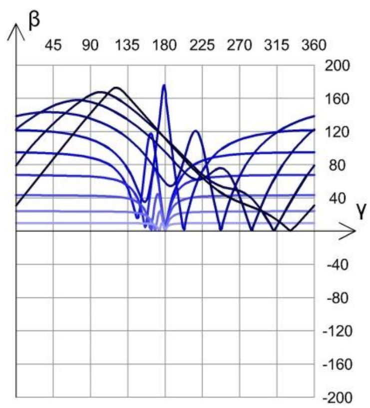 | 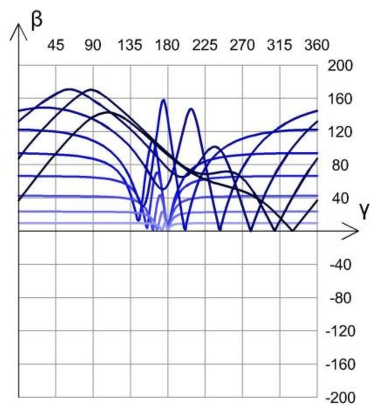 |
| $t_1$=70º and $t_2$=20º | $t_1$=80º and $t_2$=20º | $t_1$=90º and $t_2$=20º |
| 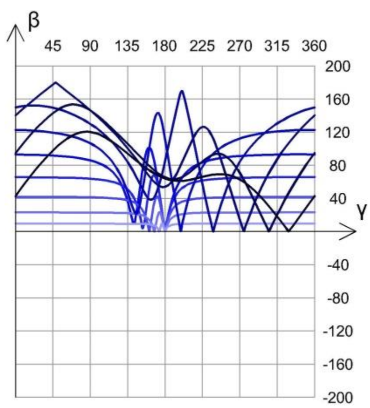 | 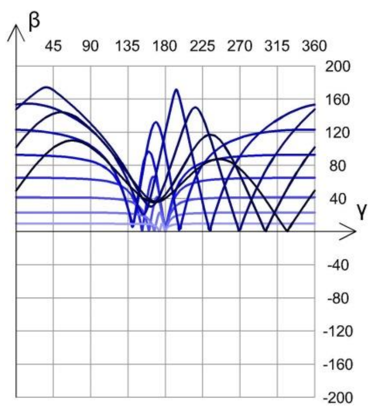 | 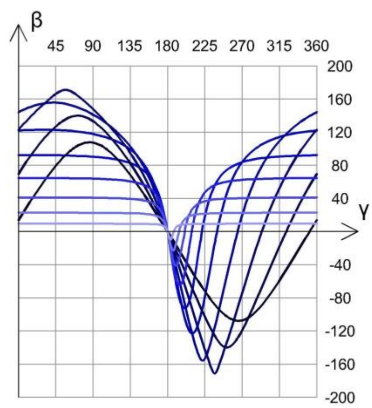 |

| | | | | |
|---|---|---|---|---|
| $b_1/a_1$=1 | $b_1/a_1$=0.9 | $b_1/a_1$=0.8 | $b_1/a_1$=0.7 | $b_1/a_1$=0.6 |
| $b_1/a_1$=0.5 | $b_1/a_1$=0.4 | $b_1/a_1$=0.3 | $b_1/a_1$=0.2 | $b_1/a_1$=0.1 |

**Table 3.** Evolution of the orientation of the scissors with a value of "t" fixed at 20°.

As can be observed in Table 3, the graphics only cut the horizontal axis two times in two cases: for $t_1 = t_2$ and for $t_1 \neq t_2$ but with one value of “t” equal to 90 °.

In the rest of the cases, the graphics only cut the horizontal axis once (the trivial solution). On the other hand, the case of $t_1 = t_2$ and of $t_1 \neq t_2$ but with one value of “t” equal to 90 ° have been already studied in Table 2 (planes and cylinders with a simple curvature).

Consequently, the only case that shall be analysed is $t_1 = t_2$. If both angles ($t_1$ and $t_2$) have the same value, there is symmetry in the original scissors and in the final scissors. This situation means that the curvature of the deployable surface is going to be constant (in the next module, the scissors are going to be the same with the same rotation between them). The only surface that has a constant curvature in all of its points is a sphere. Likewise, this deployable structure with the shape of a sphere must have polar units because it has been demonstrated that only flat deployable structures are possible for $t_1 = t_2 = 90°$.

If the study of Table 3 is done for the interval from 90° to 180°, the number of intersections with the horizontal axis will be the same but with different positions. This part of the study has been removed to avoid an excessive quantity of tables.

For $t_1 = t_2$, both original scissors are the same and, in consequence, there is a relationship between them of a rotation (the condition of $L = 2*a_1$ is not mandatory). Some application examples can be observed in Fig. 21, Fig. 22 and Fig. 23 using different relationships between L and $a_1$.

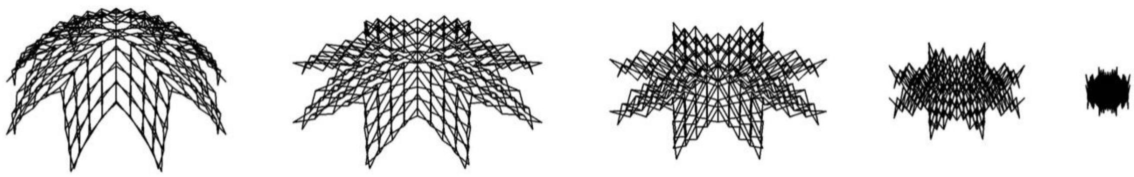

**Fig. 21.** Deployable structure with the shape of a sphere and with all elements of the same length ($L = 0.75*2*a_1$)

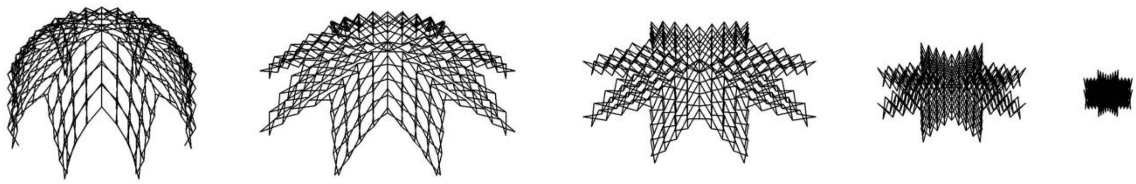

**Fig. 22.** Deployable structure with the shape of a sphere and with all elements of the same length ($L = 2*a_1$)

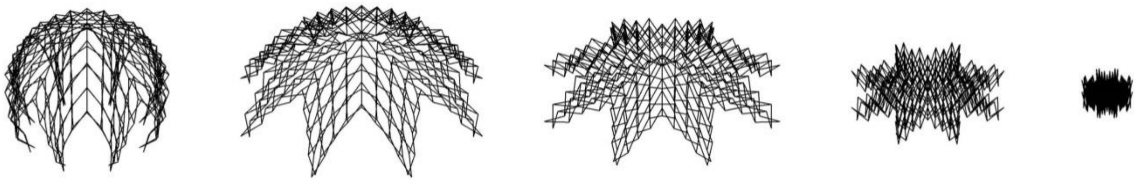

**Fig. 23.** Deployable structure with the shape of a sphere and with all elements of the same length ($L = 1.25*2*a_1$)

## 6. Results:

The goal of this section is to evaluate the influence of using elements with identical length in terms of structural behaviour. To achieve that, two spherical deployable structures are going to be designed where one model (Model A) is going to have all elements with the same length (length = 1.675 meters) and the other model (Model B) is going to have elements with a no identical length. The conditions of the simulation are going to be the next:

a) Design conditions:

- Both models will have a distance between supports of 10 meters.
- Both models will have the same number of joints.
- Both models will have the same number of elements.

b) Calculation conditions:

- Both models will have the same weight of elements, tendons and textile. Consequently, the price of both models will be the same.
- Both models will have the same cross section for the elements, tendons and textile.
- Both models will satisfy the maximum vertical displacement expected in the Spanish regulation of structures against a vertical load of 1 kN/m$^2$ applied on the surface of the structure.

Model A (all elements with an identical length) (black colour = elements and red colour = tendons) (Fig. 24):

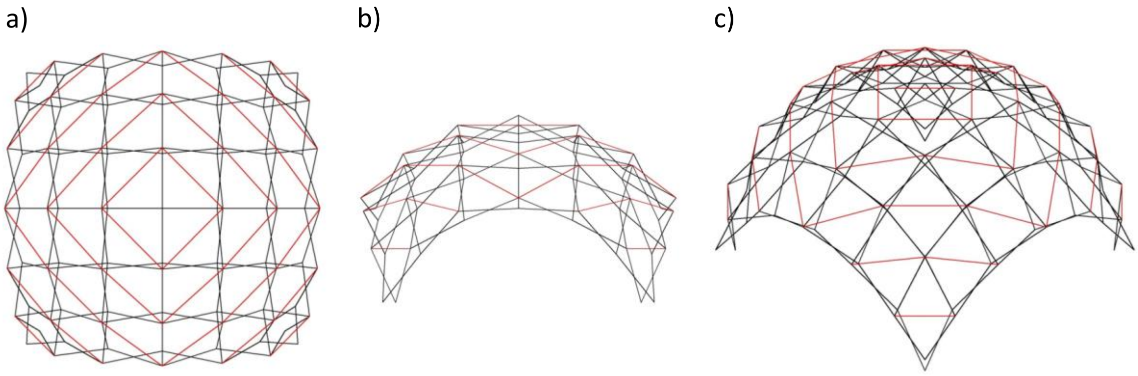


**Fig. 24.** (a) Floor view of Model A; (b) Frontal view of Model A; (c) Perspective view of Model A.

Model B (all elements with a different length) (black colour = elements and red colour = tendons) (Fig. 25):

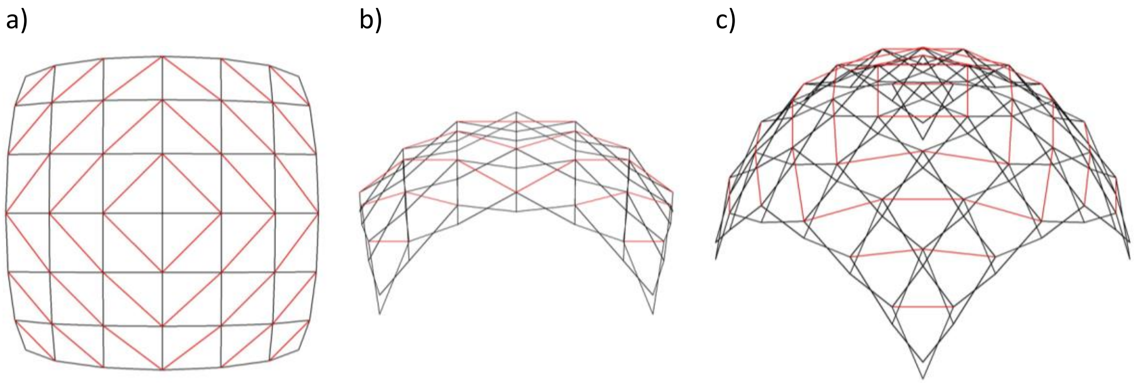


**Fig. 25.** (a) Floor view of Model B; (b) Frontal view of Model B; (c) Perspective view of Model B.

6.1. Material and section properties (Table 4 and Table 5):

| | Material | Weight per unit volume (kN/m$^3$) | Coefficient of Poisson | Modulus of elasticity (kN/m$^2$) |
|---|---|---|---|---|
| Elements | Aluminium | 26.6018 | 0.33 | 69637055 |
| Tendons | Cable | 76.9729 | 0 | $1.965 \times 10^8$ |
| Surface | Textile | 12.027 | 0.3 | 1 |

**Table 4.** Material properties.

| | Profile | Outside diameter (cm) | Wall thickness (cm) |
|---|---|---|---|
| Elements | Hollow-circular | 6 | 0.8 |
| Tendons | Solid-circular | 1 | - |
| Surface | Shell | - | 0.053 |

**Table 5.** Section properties.

6.2. Weight and price of each model (Table 6):

| | Weight of the elements (kg) | Weight of the tendons (kg) | Weight of the textile (kg) | Price of the structure (joints not included) |
|---|---|---|---|---|
| Model A | 897.66 | 43.35 | 55.37 kg | 1703.31 $ |
| Model B | 900.13 | 41.82 | 54.14 kg | 1697.68 $ |

**Table 6.** Weight and price of the structure of each model.

6.3. Vertical displacements:

a) Model A (all elements with the same length) (Fig. 26):

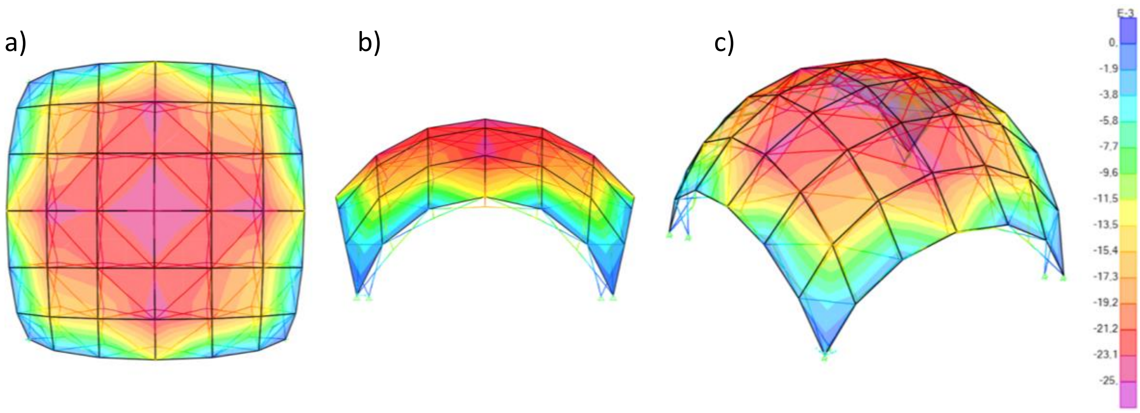


**Fig. 26.** Vertical displacements of the structure with the same length in all elements (scale in meters). (a) Floor view; (b) Frontal view; (c) Perspective view.

b) Model B (all elements with a different length) (Fig. 27):

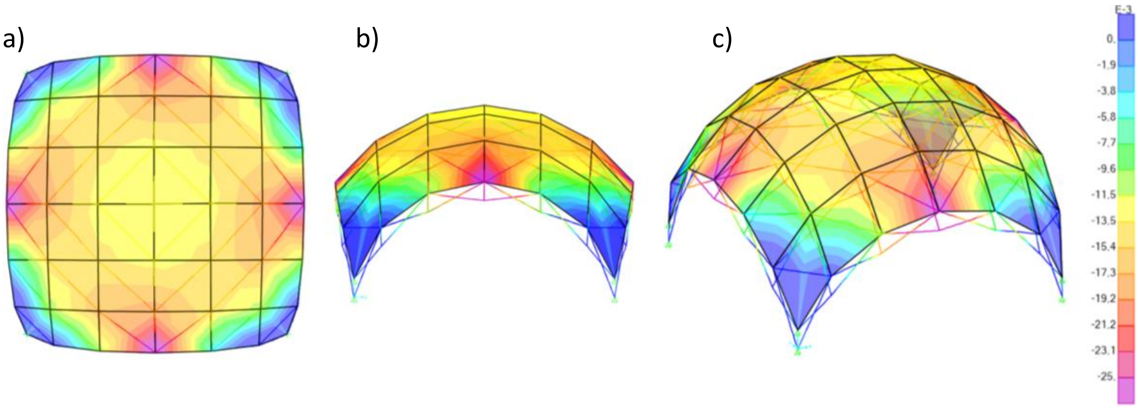


**Fig. 27.** Vertical displacements of the structure with a different length in all elements (scale in meters). (a) Floor view; (b) Frontal view; (c) Perspective view.

The comparison of the vertical displacements is represented in Figure 28:

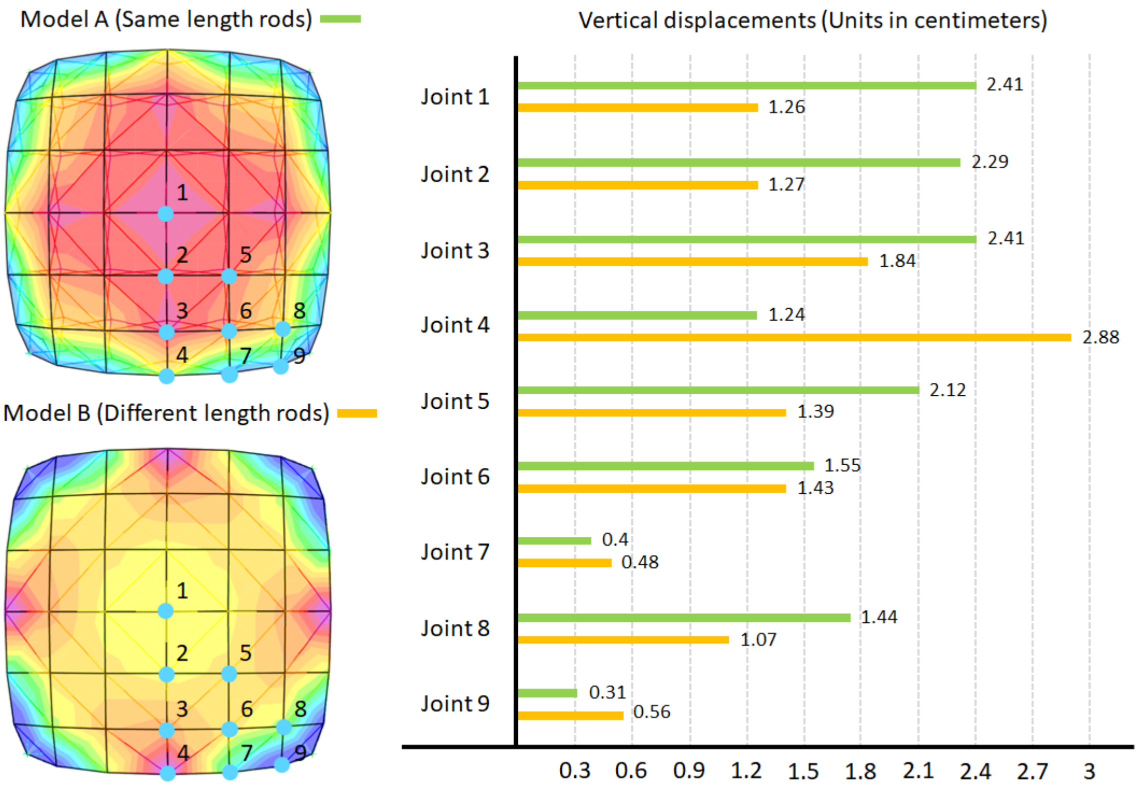


**Fig. 28.** Comparison of vertical displacements between both models (superior joints).

In addition, the limit of the vertical displacements in function of the Spanish regulation for structures is:

$$\frac{2 \cdot \text{Distance between point A and point B}}{3} \geq \text{Vert. displac. of point A} - \text{Vert. displac. of point B} \qquad (38)$$

The previous equation must be satisfied for all possible combinations of the points of the structure. The worst combination for the Model A is: Point A = Joint 6; Point B = Joint 7 and distance between point A and point B = 1.75 meters

Consequently:

$$\frac{2 \cdot 1.75}{3} \geq 1.55 - 0.4 \rightarrow 1.16 \geq 1.15 \qquad (39)$$

The worst combination for the Model B is: Point A = Joint 4; Point B = Joint 3 and distance between point A and point B = 1.59 meters

Consequently:

$$\frac{2 \cdot 1.59}{3} \geq 2.88 - 1.84 \rightarrow 1.06 \geq 1.04 \qquad (40)$$

As can be observed in Figure 28, the behaviour of the Model A (all elements with the same length) in terms of vertical displacements is worse in comparison with the Model B (all elements with a different length): only 3 points (joints 4, 7 and 9) have a lower vertical deformation in the Model A. In conclusion, the vertical displacements of a spherical deployable structure using the same length in all elements are worse in comparison with the use of elements with a different length.

6.4. Natural frequencies:

The natural frequencies of both models are:

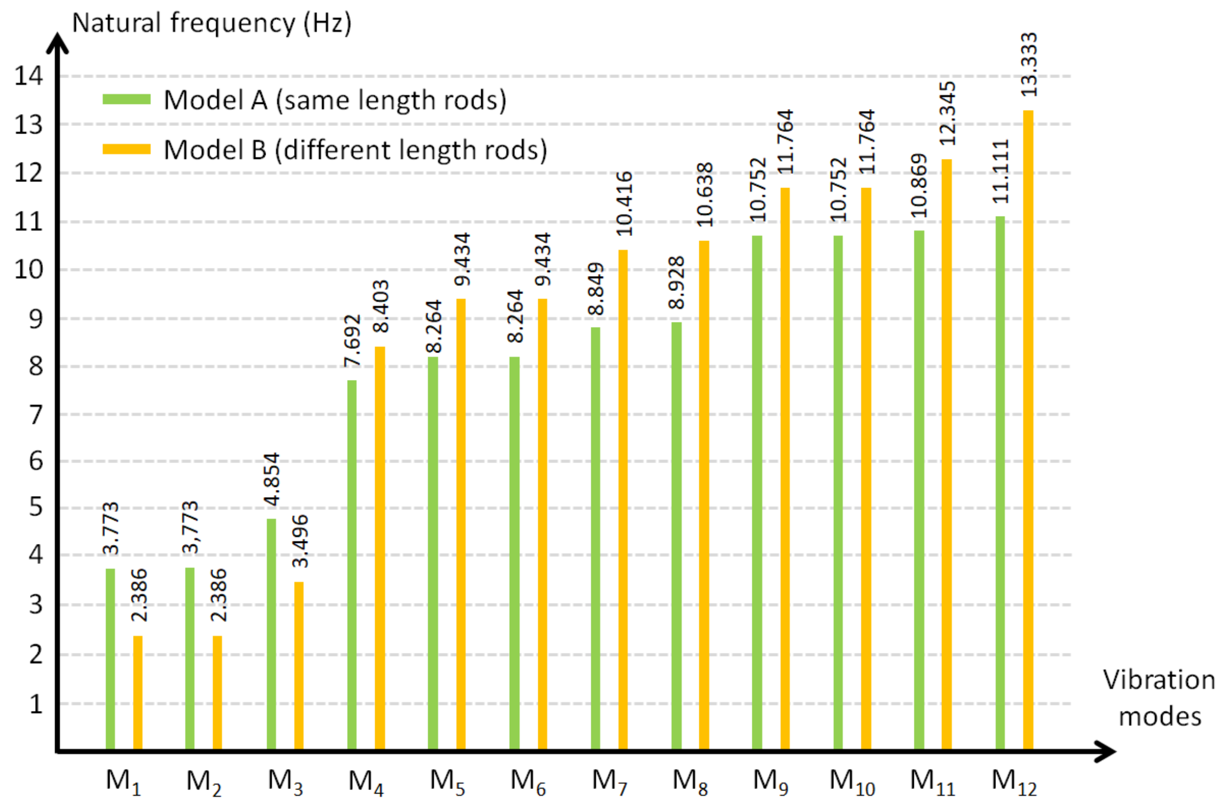


**Fig. 29.** Natural frequencies and vibration modes for each model.

When the rigidity of a structure is evaluated, $M_1$, $M_2$ and $M_3$ are always the most important vibration modes and, as can be observed in Figure 29, the Model A has a better value of the natural frequencies in $M_1$, $M_2$ and $M_3$ (the higher is the natural frequency, the higher is the rigidity of the structure).

Therefore, the behaviour of Model A against the loss of stiffness is approximately 40% - 60% better than Model B and, in consequence, the rigidity of a deployable structure using the same length in all elements is better in comparison with the use of elements with a different length.

## 7. Conclusions:

The design possibilities and the structural behaviour of deployable structures with identical elements is a topic that had been never researched in deep. The results of this paper give an overview of the geometries that can be developed using identical elements: flat shapes, cylinders with any generatrix, spheres and combinations of these options. Furthermore, the use of this geometric constraint allows the creation of deployable structures with higher vertical deformations and natural frequencies (better stability of the structure against horizontal displacements). Having these parameters in consideration, the decision of using identical elements will be based on the requirements of the structure in terms of the geometric complexity and the structural regulation of the country.

## 8. Acknowledgements and formatting of funding sources

This research did not receive any specific grant from funding agencies in the public, commercial, or not-for-profit sectors.

## 9. References:

[1] Jiten Patel, G.K. Ananthasuresh, A kinematic theory for radially foldable planar linkages, International Journal of Solids and Structures, Volume 44, 2007, pp. 6279-6298, https://doi.org/10.1016/j.ijsolstr.2007.02.023

[2] K. Roovers, N. De Temmerman, Deployable scissor grids consisting of translational units, International Journal of Solids and Structures, Volume 121, 2017, pp. 1-17, https://doi.org/10.1016/j.ijsolstr.2017.05.015

[3] Roovers, Kelvin & Temmerman, Niels, Geometric Design of Deployable Scissor Grids Consisting of Generalized Polar Units. Journal of the International Association for Shell and Spatial Structures, Volume 58, 2017, pp. 227-238, https://doi.org/10.20898/j.iass.2017.193.865

[4] Yao Chen, Jian Feng, Folding of a type of deployable origami structures, International Journal of Structural Stability and Dynamics, Volume 12, 2013, pp. 1-17, https://doi.org/10.1142/S021945541250054X

[5] Sicong Liu, Lv Weilin, Guoxing Lu, Deployable Prismatic Structures With Rigid Origami Patterns, Journal of Mechanisms and Robotics, Volume 8, 2015, pp. 1-33, https://doi.org/10.1115/1.4031953

[6] Zirui Zhai, Yong Wang, Hanqing Jiang, Origami-inspired, on-demand deployable and collapsible mechanical metamaterials with tunable stiffness, Proceedings of the National Academy of Sciences, Volume 115, 2018, pp. 1-6, https://doi.org/10.1073/pnas.1720171115

[7] Lishuai Jin, Antonio Elia Forte, Bolei Deng, Ahmad Rafsanjani, Katia Bertoldi, Kirigami-Inspired Inflatables with Programmable Shapes, Advanced Materials, 2020, pp. 1-41, https://doi.org/10.1002/adma.202001863

[8] Sahab Babaee, Simo Pajovic, Ahmad Rafsanjani, Yichao Shi, Katia Bertoldi, Giovanni Traverso, Bioinspired kirigami metasurfaces as assistive, Nature Biomedical Engineering, 2020, pp. 1-30, https://doi.org/10.1038/s41551-020-0564-3

[9] Félix Candela, Emilio Pérez Piñero, Santiago Calatrava, Félix Escrig, Juan Pérez Valcárcel, Arquitectura Transformable (Transformable Architecture), Seville Higher Technical School of Architecture, 1993, ISBN: 84-600-8583-X

[10] Yan Chen, Zhong You, Tibor Tarnai, Threefold-symmetric Bricard linkages for deployable structures, International Journal of Solids and Structures, Volume 42, 2005, pp. 2287-2301, https://doi.org/10.1016/j.ijsolstr.2004.09.014

[11] E. Pérez Piñero, Teatros Desmontables (Deployable Theaters), Informes de la Construcción, Volume 24, June 1971, pp. 34-42, https://doi.org/10.3989/ic.1971.v24.i231.3360

[12] F. Escrig, Modular, Ligero, Transformable: Un Paseo Por La Arquitectura Ligera Móvil (Modular, Lightweight, Transformable: A Walk Through Mobile Lightweight Architecture), Universidad De Sevilla, Sevilla, 2012, ISBN: 978-84-472-1427-3

[13] F. Escrig, J.P. Valcárcel, Geometry of expandable space structures, International Journal of Space Structures, Volume 8, 1993, pp. 71–84, https://doi.org/10.1177/0266351193008001-208

[14] A. Fomin, L. Dvornikov, M. Paramonov, A. Jahr, To the theory of mechanisms subfamilies, International Conference on Mechanical Engineering, Automation and Control Systems 2015 (MEACS2015), Volume 124, 2015, pp. 1-4, https://doi.org/10.1088/1757-899x/124/1/012055

[15] A. Fomin, L. Dvornikov, J. Paik, Calculation of General Number of Imposed Constraints of Kinematic Chains, International Conference on Industrial Engineering, Volume 206, 2017, pp. 1309-1315, https://doi.org/10.1016/j.proeng.2017.10.636

[16] L. Sánchez-Cuenca, Cupula Extensible (Deployable Dome), Revista de Edificación, Volume 23, 1996, pp. 43-47, https://hdl.handle.net/10171/16703

[17] L. Sánchez-Cuenca, Geometric models for expandable structures, Transactions on the Built Environment, Volume 21, 1996, pp. 93-102, DOI: 10.2495/MRS960091

[18] J. Gantes Charis, Deployable Structures: Analysis and Design, WIT Press, 2001, ISBN: 1-85312-660-8

[19] L. I. W. Arnouts, T. J. Massart, N. De Temmerman, P. Z. Berke, Computational modelling of the transformation of bistable scissor structures with geometrical imperfections. Engineering Structures, Volume 177, 2018, pp. 409-420, https://doi.org/10.1016/j.engstruct.2018.08.108

[20] C.J. Gantes, E. Konitopoulou, Geometric design of arbitrarily curved bi-stable deployable arches with discrete joint size, International Journal of Solids and Structures, Volume 41, 2014, pp. 5517-5540, https://doi.org/10.1016/j.ijsolstr.2004.04.030

[21] C. Hoberman, 1991. Reversibly expandable doubly-curved truss structure. US Patent. Number: 4.942.700.

[22] Z. You and S. Pellegrino, Foldable bar structures, International Journal of Solids and Structures, Volume 34, 1997, pp. 1825-1847, https://doi.org/10.1016/S0020-7683(96)00125-4

[23] Carlos J. García-Mora, Jose Sánchez-Sánchez, Geometric method to design bistable and non - bistable deployable structures of straight scissors based on the

convergence surface, University of Seville, April 2020, vol. 146, Mechanism and Machine Theory, pp. 1-31, https://doi.org/10.1016/j.mechmachtheory.2019.103720

[24] Carlos J. García-Mora, Jose Sánchez-Sánchez, The convergence surface method for the design of deployable scissor structures. Automation in Construction. University of Seville, February 2021, vol. 122, pp. 1-19, https://doi.org/10.1016/j.autcon.2020.103488